Energy 318 (2025) 134845

Contents lists available at ScienceDirect

Energy

journal homepage: www.elsevier.com/locate/energy

Enhancing sustainability in cement manufacturing through waste heat recovery and CCHP systems

Mahdi Mahmoudkhani [a], Alibakhsh Kasaeian [b,*], Narges Sadat Nazari [c], Fatemeh Afshari [d], Mehdi Esmaeili Bidhendi [a]

[a] Faculty of Environment, University of Tehran, Tehran, Iran
[b] Faculty of New Sciences and Technologies, University of Tehran, Tehran, Iran
[c] School of Chemical, Petroleum and Gas Engineering, Iran University of Science and Technology, Tehran, Iran
[d] Chemical Engineering Department, Amirkabir University of Technology (Tehran Polytechnique), Tehran, Iran

ARTICLE INFO

Keywords:
Waste heat recovery
Cement
CCHP
Steam rankine cycle
4E analysis

ABSTRACT

The cement industry's rapid expansion has resulted in heightened environmental and economic issues due to significant greenhouse gas emissions and energy losses. Conventional manufacturing methods, which often release waste heat, significantly increase carbon emissions. This paper proposes an innovative combined cooling, heating, and power (CCHP) system that enables significant waste heat recovery. Through a Steam Rankine Cycle and a Li-Br absorption chiller, the system generates power, heating, and cooling, effectively repurposing thermal energy otherwise wasted. This study provides a comprehensive 4E (energy, exergy, economic, and environmental) analysis, demonstrating the system's potential to significantly improve sustainability in cement production by enhancing resource efficiency and reducing carbon emissions. Our model, validated with accurate operational data and simulated through EES software, demonstrates significant improvements in energy and exergy efficiencies. Based on the input data and operational results, the proposed system recovers 3078 kW of helpful energy, including 945 kW of cooling and 2133 kW of heating. The system's energy and exergy efficiency are 30.2 % and 28.69 %, respectively, and with an initial investment of $661,803, the payback period is 6.183 years. Additionally, the sustainability index is 0.1216, and the exergoenvironmental index is 0.6928, reflecting the ecological and economic viability of the system.

Abbreviations

4E	Energy, Exergy, Economic, and Environmental
CCHP	Combined Cooling, Heat and Power
CCPPs	Combined Cycle Power Plants
CHP	Combined Heat and Power
CRF	Capital Recovery Factor
CSI	Cement Sustainability Initiative
DHW	Domestic Hot Water
DUC	Damage Unit Cost
EES	Engineering Equation Solver
EXV1	Expansion Valve 1
EXV2	Expansion Valve 2
GHG	Greenhouse Gases
HEX	Heat Exchanger
HRSG	Heat Recovery Steam Generator
IEA	International Energy Agency

(*continued on next column*)

(*continued*)

4E	Energy, Exergy, Economic, and Environmental
ORC	Organic Rankine cycle
PB	Payback Period
SPC	Space Cooling
SPH	Space Heating
SRC	Steam Rankine cycle
WHR	Waste Heat Recovery
Nomenclature	
$\dot{C}_{env}$	Cost rate of environmental penalty ($/hr)
$\dot{C}_{f,k}$	Fuel cost rate of kth equipment ($/hr)
$\dot{C}_{p,k}$	Product cost rate of kth equipment ($/hr)
$c_{f,k}$	Fuel cost of kth equipment ($)
$c_{i,k}$	Exergy cost of kth equipment ($)
$c_{p,k}$	Product cost of kth equipment ($)
$c_{q,k}$	Heat transfer exergy cost of kth equipment ($)

(*continued on next page*)

* Corresponding author.
E-mail address: akasa@ut.ac.ir (A. Kasaeian).

https://doi.org/10.1016/j.energy.2025.134845
Received 4 September 2024; Received in revised form 22 November 2024; Accepted 3 February 2025
Available online 4 February 2025

(continued)

4E	Energy, Exergy, Economic, and Environmental
$c_{w,k}$	Useful work exergy cost of kth equipment ($)
$\dot{E}_{Cooling}$	Output cooling generated rate (kJ/s)
$\dot{E}_{Heating}$	Output heat generated rate (kJ/s)
$\dot{E}_{hot\ gas}$	Hot gas energy rate (kJ/s)
$\dot{E}x_{ch}$	Chemical exergy rate (kJ/s)
$\dot{E}x_{Cooling}$	Cooling exergy rate (kJ/s)
$\dot{E}x_{D}$	Exergy of destruction rate (kJ/s)
$\dot{E}x_{f,k}$	Fuel exergy rate of kth equipment (kJ/s)
$\dot{E}x_{Heating}$	Heating exergy rate (kJ/s)
$\dot{E}x_{in}$	Input exergy rate (kJ/s)
$\dot{E}x_{ki}$	Kinetic exergy rate (kJ/s)
$\dot{E}x_{p,k}$	Product exergy rate of kth equipment (kJ/s)
$\dot{E}x_{ph}$	Physical exergy rate (kJ/s)
$\dot{E}x_{po}$	Potential exergy rate (kJ/s)
$\dot{E}x_{Q}$	Exergy of heat transfer rate (kJ/s)
$\dot{E}x_{q,k}$	Exergy of heat transfer rate of kth equipment (kJ/s)
$\dot{E}x_{tot}$	Rate of total exergy (kJ/s)
$\dot{E}x_{W}$	Exergy of work done rate (kJ/s)
ex_{i}	Input exergy (kJ/kg)
ex_{o}	Output exergy (kJ/kg)
ex_{ph}	Physical exergy (kJ/kg)
f_{ei}	Exergo-environmental index
f_{es}	Exergo-environmental stability
h_{i}	Input enthalpy (kJ/kg)
h_{o}	Output enthalpy (kJ/kg)
$\dot{m}_{i}$	Rate of input mass (kg/s)
$\dot{m}_{o}$	Rate of output mass (kg/s)
P_{0}	Standard reference pressure (kPa)
$\dot{Q}$	Heat exchanged rate (kJ/s)
Q_{L}	Heat loss (kJ)
T_{0}	Standard reference temperature (°C)
$\dot{W}$	Work done rate (kJ/s)
$\dot{W}_{k}$	Work done rate of kth equipment (kJ/s)
$\dot{W}_{turb}$	Output power generated rate (kJ/s)
$\dot{Z}_{k}$	Capital investment cost of kth equipment rate ($/hr)
Z_{k}	Capital investment cost of kth equipment ($)
Greek	
θ_{ei}	Exergo-environmental improvement
θ_{est}	Exergo-environmental sustainability
ε_{E}	Energy efficiency
ε_{Ex}	Exergy efficiency

1. Introduction

The cement industry stands as a cornerstone of global infrastructure, yet it is also a significant contributor to greenhouse gas (GHG) emissions, particularly carbon dioxide (CO_2) [1,2]. In the GCAA report, different independent sources estimated that cement manufacturing caused between 5 % and 8 % of the global GHG emissions. As our population grows and urbanizes, the demand for cement is projected to increase substantially. According to the IEA CSI Cement Technology Roadmap, global cement production is expected to rise by 12–23 % by 2050.

Modern industry relies on cement production, but it creates considerable environmental and economic challenges [3,4]. Waste heat generated during the production process is one of the significant issues. This heat, often released into the atmosphere, represents a substantial energy loss and contributes to the industry's carbon footprint [5]. However, recovering and efficiently utilizing this wasted heat could transform the industry [6]. Waste heat recovery programs provide an innovative solution for reducing energy loss, lowering operational expenses, and minimizing environmental impact [7]. Heat recovery technologies can be categorized into three main categories: recovering heat for lower-quality applications, upgrading heat, and converting heat into electricity [8]. These technologies significantly improve energy efficiency and sustainability within the cement industry by capturing and recovering heat generated in cement plants [9].

Several studies have explored various aspects of WHR in cement plants, focusing on different technologies and methodologies [10]. For example, research on optimizing power generation assets in industrial settings has highlighted the economic benefits and enhanced efficiency of integrating advanced WHR strategies into existing infrastructures [11]. Similarly, studies on cogeneration plants, such as the power-augmented steam power plant in cement factories, illustrate significant improvements in electrical efficiency and heat recovery [12]. According to Ghalandari et al. [13], energy analysis for thermal processing units of cement plants of a new generation demonstrated the possibility of converting waste heat to energy savings. A performance evaluation of novel waste heat recovery designs incorporating coal-fired power plants, conducted by Chen et al. [14], has also shown promising results in improving overall energy efficiency. In additional efforts, Jamali and Noorpoor [15] optimized a WHR plant to capture CO_2 and produce electricity for a cement factory by integrating biomass, solar, and waste heat. Their winter cost reduction was 24 %, and their summer exergy efficiency was 39 % higher. From an economic perspective, Brueckner et al. [16] highlighted the financial viability of WHR applications, particularly electric heat pumps and absorption chillers, which offer attractive returns on investment and shorter payback periods when operated extensively. The steam Rankine cycle is a method of converting heat into work and is most commonly used in generating electricity [17]. In a similar stance, Khurana and colleagues [18] investigated using a steam cycle to harness waste heat streams, successfully generating 4.4 MW of electricity and recovering about 30 % of the plant's electricity needs. Tang et al. [19] designed an SRC process based on high- and low-pressure steam to handle the waste heat from marine engines at different grades. A combined cycle power plant using dual-pressure SRC reduced braking fuel consumption by 6.1 %. Gomaa et al. [20] explored an Organic Rankine Cycle (ORC) integrated with hybrid solar collectors in cement plants, achieving electricity generation of 323–360 kW. Their study revealed a more extended payback period of approximately 3.75 years. The Organic Rankine Cycle converts thermal energy into mechanical work and then electricity, using organic fluids instead of water [21]. The combination of SRC with ORC is a hybrid device designed to improve overall efficiency by utilizing a broad range of heat sources [22]. According to Ozturk and Dincer [23], the overall operation could achieve higher efficiency if SRC and ORC cycles were used. The SRC optimized heat conversion at high temperatures, while the ORC recovered heat from waste heat. Freeman et al. [24] integrated thermal energy storage (TES) solutions to improve CHP efficiency by optimizing energy production, minimizing expenses, and improving operational performance. According to Karellas et al. [25], the choice between SRC and ORC relied on the temperature and specific operational conditions of the cement plant. The energetic and exergetic evaluations provided comprehensive insights into how each model performed. Cement production is energy-intensive, requiring substantial amounts of electricity and heat. The sustainability and environmental benefits of renewable energy resources make them an attractive alternative to conventional energy sources for heating and cooling [26]. Combined cooling, heat, and power techniques efficiently utilize waste heat from cement production to generate electricity, heating, and cooling. By capturing and recycling this waste heat, cement plants can achieve higher overall energy efficiency [27]. Nami et al. [28] performed a thermodynamic analysis of WHR processes, emphasizing energy and exergy efficiencies. Their study focused on applying geothermal and waste heat-fired CCHP devices for a centralized domestic heating, cooling, and power network. As an extension of CCHP models, Wang et al. [29] developed a similar approach for a cement plant, utilizing flue gas waste heat to generate electricity. This innovative approach resulted in a notable decrease in CO_2 emissions and internal energy consumption by 22.02 %. Additionally, Wang et al. [30] explored the benefits of a solar-assisted CCHP gas turbine power station, which achieved an impressive carbon emission reduction rate of about 41.0 % per unit of energy production. Although numerous studies have explored WHR methods in industrial settings,

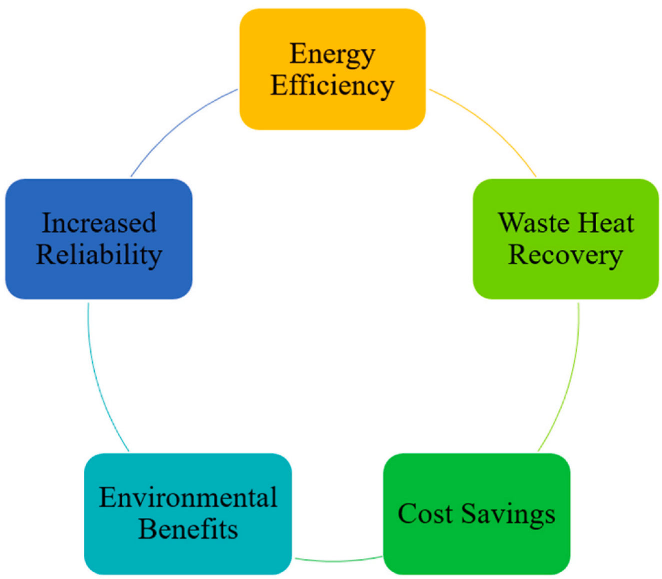

Fig. 1. Comprehensive benefits of CCHP.

existing solutions often focus on isolated aspects of energy recovery, lacking a comprehensive integration of cooling, heating, and power generation. This study addresses this gap by introducing a CCHP system tailored to the cement industry.

In this study, we analyze a steam Rankine cycle's performance using actual operational data from a specific cement plant and model it with Engineering Equation Solver (EES) software to ensure practical applicability in industrial settings. An analysis of the potential and effectiveness of the proposed method is conducted from the perspectives of energy, exergy, economics, and the environment. The study presents a novel method of simulating multiple operational conditions through detailed modeling techniques. Additionally, the detailed 4E evaluation sets this work apart from prior studies by offering a complete evaluation that addresses both technical and sustainability aspects. By incorporating extensive economic and environmental assessments, this research provides an optimized, data-driven framework for WHR integration, achieving significant energy recovery and cost reduction. These contributions ultimately position this work as a superior solution for enhancing productivity and environmental sustainability in cement manufacturing.

2. Methodology

In a cement plant, the exhaust gas of the flue is typically the part that generates the most waste heat. During the clinker production process in the kiln, raw materials are heated to high temperatures, releasing significant thermal energy. The waste heat in the form of hot gas flows out of the flue and is often vented into the atmosphere [31]. This represents a lost opportunity, as this heat energy could be harnessed for various purposes, such as power generation or preheating raw materials. Capturing and utilizing this waste heat can improve the overall energy efficiency of the cement manufacturing process. Various technologies, such as combined cooling, heat, and power (CCHP) units or waste heat recovery boilers, can capture and utilize the hot gas flow from the cement plant flue, reducing energy consumption and environmental impact.

2.1. System description

Combined Cooling, Heating, and Power (CCHP) processes are often used in industrial settings, including cement plants, for several reasons. Introducing CCHP in an article could be beneficial for several reasons.

- Energy Efficiency: CCHP operations allow for the simultaneous generation of electricity, heat, and sometimes cooling from a single energy source. This results in a more efficient use of the primary energy input, minimizing waste and increasing overall energy efficiency.
- Waste Heat Recovery: Cement plants generate significant waste heat, especially in the kiln process. CCHP methods are designed to capture and utilize this waste heat for space heating, water heating, or even additional power generation.
- Cost Savings: Using waste heat for on-site heating or cooling, CCHP units can lead to cost savings for the plant. This is particularly relevant to industrial processes where electricity and thermal energy are essential.
- Environmental Benefits: CCHP technology can contribute to a reduction in greenhouse gas emissions by optimizing the use of energy resources. The efficient use of waste heat can decrease the reliance on conventional energy sources and lower the overall environmental impact of the cement manufacturing process.
- Increased Reliability: CCHP installations can enhance the reliability of the energy supply for a cement plant. A decentralized energy source that produces electricity and heat on-site makes the plant less vulnerable to external power outages or disruptions.

Including CCHP in the introduction sets the stage for discussing how the cement plant can enhance its sustainability and energy efficiency by adopting such solutions, providing a comprehensive solution for addressing power and heat needs while minimizing environmental impact. The system configuration and operational framework are illustrated in Fig. 1.

There are several types of production in a CCHP waste heat recovery process, such as power generation, domestic cooling, and heating. To produce output, a heat source must be available until the energy demand for each section is met. As waste heat in exhausted gases from kiln streams has an appropriate temperature, it can be used as the primary heat source and distributed among components. The kiln operates in different temperature zones. The burning zone operates at 300–350 °C, the decomposition and exothermic reaction zone is 280–300 °C, and the drying and preheating zone is 240 °C. The kiln structure consists of cylinders, feeding mechanisms, supports, transmissions, and seals [32]. Energy content is distributed among the parts as the input gas passes through them, as shown in Fig. 2. In the first section, power generation, the energy of hot gas input is exchanged with the working fluid of the Rankine cycle in HRSG equipment. In the first cycle, received energy turns water into superheated steam that moves toward the turbine. Steam turbines convert mechanical energy from superheated steam into electrical energy, which can be used in numerous ways. In the domestic heating section, steam with a certain amount of thermal energy produces sensible heat (used for building heating and HVAC). To repeat this cycle, domestic heating output liquid is sent to HRSG via a pump.

It is still possible to create added value by using the output gas from the power generation heat exchanger to make consumable hot water. By using a heat exchanger that works in water heating, it can raise the temperature of water to a useable level. It is still possible to recover the amount of energy after producing domestic hot water. For this purpose, an absorption chiller apparatus is used for cooling production. As a refrigerant and absorbent, water and Li-Br are used in this module. As a combination, these two substances are pumped towards a generator. They pass through the generator and become warm until a thick mixture and water are evaporated. The steam moves towards a condenser. Upon entering a condenser, this vapor turns into saturated liquid, whose temperature drops significantly after exiting an expansion valve and plays a crucial role in cooling production when in contact with incoming air at SPC. Additionally, the absorbent moves toward the absorber while cooling is taking place.

The studied waste gas with a temperature of 250 °C, pressure of 1.013 atm, and a mass flow rate of 18.43 kg/s is entered in stream No. 1

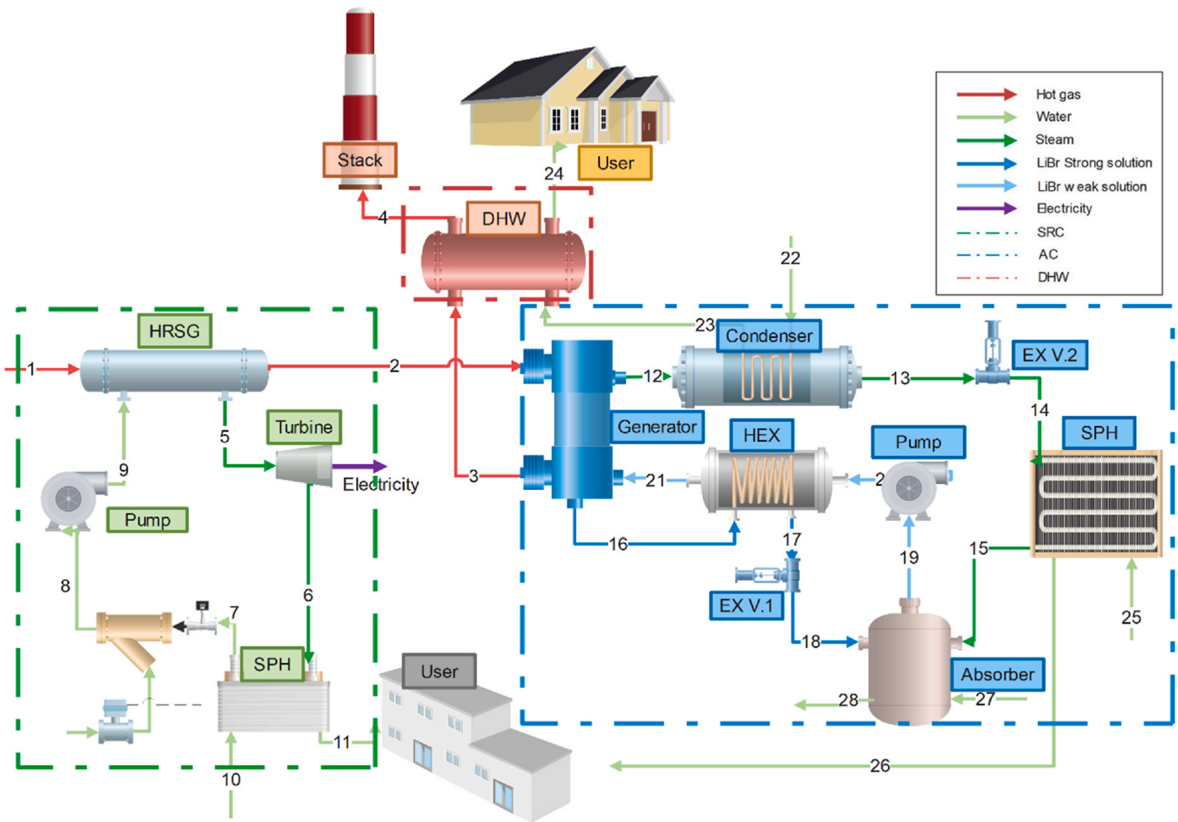

Fig. 2. Schematic of CCHP process in cement plant.

Table 1
Input variables for thermodynamic modeling [33–36].

Parameters	Value
Ambient temperature (°C)	25
Ambient pressure (kPa)	101.3
Condenser pressure of SRC (kPa)	15
Boiler pressure of SRC (kPa)	410
HRSG efficiency (%)	95
Turbine isentropic efficiency (%)	90
Electricity generator efficiency (%)	95
Output steam quality of turbine (%)	90
Pumps isentropic efficiency (%)	85
SPH efficiency (%)	95
Flow rate of steam Rankine cycle (kg/s)	3.8
SPH output temperature (°C)	45
SRC pump efficiency (%)	95
Absorber pressure (kPa)	0.8726
Generator pressure of SRC (kPa)	5.627
The flow rate of the mixture in the adsorption chiller (kg/s)	34.5
Generator temperature (°C)	80
HEX efficiency (%)	60
SPC efficiency (%)	95
DHW pinch point (°C)	7
Cooling inlet stream temperature (°C)	25
Cooling outlet stream temperature (°C)	12
heating inlet stream temperature (°C)	25
heating outlet stream temperature (°C)	38

according to the schematic of Fig. 2. The percentage composition of the input gas is: 68.9 % N_2, 22.5 % CO_2, 5.8 % H_2O, 1.1 % O_2, 1 % Ar, and 0.7 % SO_2 [33]. This information gives insight into the characteristics of the waste gas stream, which is essential for assessing its potential for waste heat recovery or other utilization methods in the cement manufacturing process.

For the simulation, we employed the Engineering Equation Solver (EES), a powerful equation solver widely used in engineering, particularly for thermodynamic calculations. Its robust thermodynamic library provides highly accurate data. Based on the governing thermodynamic relationships detailed in the following sections, each subsystem was modeled. These relationships include energy, exergy, and exergoeconomic balance equations, individually applied to each component, with subsystems interconnected through streams. Ultimately, efficiency formulas and output rates for each subsystem were applied based on system inputs and outputs.

Several assumptions were made in the formulation of our model. First, a constant cement production rate was assumed, given that fluctuations in this rate would introduce a separate variable beyond the scope of this study. Second, a steady-state approach was adopted to facilitate a clear understanding of the system's behavior under varying conditions. This assumption allowed for the modeling of uniform fluid distribution within each subsystem. Furthermore, to isolate the effects of the variables of interest, energy losses due to non-ideal gas behavior and heat losses along the system were disregarded. By simplifying the model in this manner, the specific impacts of the investigated parameters could be focused on. The ambient temperature and pressure adopted for this study were 25 °C and 101.3 kPa, respectively. The water inlet temperature, serving both heating and cooling requirements, was equated to the ambient temperature. The corresponding outlet temperatures were fixed at 12 and 38 °C. Input variables for thermodynamic modeling of HRSG are presented in Table 1 with their references.

2.2. *Energy analysis*

Energy analysis is essential for an understanding of dynamics within any mechanism. It provides valuable insight into the interaction between mass and energy in any kind of energy exchange. In this section, the basic principles of energy balance are discussed and explained by the first law of thermodynamics. The first step in this direction is to use the conservation principles of mass and energy as a foundation. We establish

Table 2
Energy balance equation for the components of the proposed CCHP unit.

Component	Energy Balance Equations	Eq. No.
HRSG	$\dot{E}_1 - \dot{E}_2 = \dot{E}_5 - \dot{E}_9$	(3)
Turbine	$\dot{W}_{turb} = \dot{E}_6 - \dot{E}_5$	(4)
Space heating	$\dot{E}_6 - \dot{E}_7 = \dot{E}_{11} - \dot{E}_{10}$	(5)
Pump	$\dot{W}_{p1} = \dot{E}_9 - \dot{E}_8$	(6)
Heat generator	$\dot{E}_3 - \dot{E}_4 = \dot{E}_{12} + \dot{E}_{16} - \dot{E}_{21}$	(7)
Condenser	$\dot{E}_{12} - \dot{E}_{13} = \dot{E}_{23} - \dot{E}_{22}$	(8)
Expansion valve1	$\dot{E}_{13} = \dot{E}_{14}$	(9)
Evaporator	$\dot{E}_{15} - \dot{E}_{14} = \dot{E}_{25} - \dot{E}_{26}$	(10)
ABS	$\dot{E}_{28} - \dot{E}_{27} = \dot{E}_{18} + \dot{E}_{15} - \dot{E}_{19}$	(11)
Pump2	$\dot{W}_{p1} = \dot{E}_{20} - \dot{E}_{19}$	(12)
HEX	$\dot{E}_{16} - \dot{E}_{17} = \dot{E}_{21} + \dot{E}_{20}$	(13)
Expansion valve2	$\dot{E}_{17} = \dot{E}_{18}$	(14)
DHW	$\dot{E}_2 - \dot{E}_3 = \dot{E}_{24} - \dot{E}_{23}$	(15)

Table 3
Exergy balance equation for the components of the proposed CCHP unit.

Component	Exergy Balance Equations	Eq. No.
HRSG	$\dot{E}x_{D,HRSG} = (\dot{E}x_1 + \dot{E}x_9) - (\dot{E}x_2 + \dot{E}x_5)$	(26)
Turbine	$\dot{E}x_{D,Turbine} = \dot{E}x_5 - (\dot{E}x_6 + \dot{W}_{turb})$	(27)
Space heating	$\dot{E}x_{D,SPH} = (\dot{E}x_6 + \dot{E}x_{10}) - (\dot{E}x_7 + \dot{E}x_{11} + \dot{E}x_D)$	(28)
Pump1	$\dot{E}x_{D,P_1} = (\dot{E}x_8 + \dot{W}_{p1}) - \dot{E}x_9$	(29)
Heat generator	$\dot{E}x_D = (\dot{E}x_3 + \dot{E}x_{21}) - + \dot{E}x_{12} + \dot{E}x_{16})$	(30)
Condenser	$\dot{E}x_D = (\dot{E}x_{22} + \dot{E}x_{12}) - (\dot{E}x_{23} + \dot{E}x_{13})$	(31)
Expansion valve	$\dot{E}x_D = \dot{E}x_{13} - \dot{E}x_{14} = T_0.m_{13}(s_{13} - s_{14})$	(32)
Evaporator	$\dot{E}x_D = (\dot{E}x_{14} + \dot{E}x_{25}) - (\dot{E}x_{15} + \dot{E}x_{26})$	(33)
ABS	$\dot{E}x_D = (\dot{E}x_{27} + \dot{E}x_{15} + \dot{E}x_{18}) - (\dot{E}x_{28} + \dot{E}x_{19})$	(34)
Pump2	$\dot{E}x_D = \left(\dot{E}x_{19} + \dot{W}_{p1}\right) - \dot{E}x_{20}$	(35)
HEX	$\dot{E}x_D = (\dot{E}x_{16} + \dot{E}x_{20}) - (\dot{E}x_{17} + \dot{E}x_{21})$	(36)
Expansion valve	$\dot{E}x_D = \dot{E}x_{13} - \dot{E}x_{14} = T_0.m_{13}(s_{13} - s_{14})$	(37)
DHW	$\dot{E}x_D = (\dot{E}x_2 + \dot{E}x_{23}) - (\dot{E}x_3 + \dot{E}x_{24})$	(38)

the foundation through comprehensive equations governing the overall mass and energy balances, ensuring a holistic view of the process's behavior. By employing a systematic control volume analysis, we have developed individualized energy balance equations for key components such as pumps, heat exchangers, evaporators, and condensers. This approach involves defining a control volume around each component and applying the conservation of mass and energy principles to quantify the energy interactions across its boundaries. By carefully selecting the control surfaces and accounting for all energy transfers, including heat, work, and energy associated with mass flow, we have been able to precisely determine the energy performance of each component and the overall system. The direct application of the control volume method has enabled us to isolate and analyze the energy losses and gains within the system, providing valuable insights for optimization and improvement. The general form of the conservation of mass equation for any operation:

$$\sum \dot{m}_i = \sum \dot{m}_o \tag{1}$$

The energy conservation equation, derived from the first law of thermodynamics under the assumption of a steady state, is expressed as:

$$\sum \dot{m}_i h_i + \dot{Q} = \sum \dot{m}_o h_o + \dot{W} \tag{2}$$

Where $\dot{m}_i$ and $\dot{m}_o$ are input and output mass rate, h_i and h_o are input and output enthalpy, $\dot{Q}$ is heat exchanged rate, and $\dot{W}$ is work done rate. Energy balance equations around all equipment must be written (mass balance too, optional), and they are gathered in Table 2 to be compared with each other.

To obtain the performance of the desired method from the perspective of the first law of thermodynamics, the energy efficiency formula is used as follows:

$$\varepsilon_E = \frac{\dot{W}_{net} + \dot{E}_{Cooling} + \dot{E}_{Heating}}{\dot{E}_{Hot\ gas}} \tag{16}$$

$$\dot{W}_{net} = \dot{W}_{turb} - \dot{W}_{pump} \tag{17}$$

$$\dot{E}_{Cooling} = \dot{m}_{25}(h_{25} - h_{26}) \tag{18}$$

$$\dot{E}_{Heating} = \dot{m}_{10}(h_{11} - h_{10}) \tag{19}$$

$$\dot{E}_{Hot\ gas} = \dot{m}_1(h_1 - h_2) \tag{20}$$

$\dot{W}_{turb}$, $\dot{E}_{Cooling}$, $\dot{E}_{Heating}$ represent heat production, cooling, and power generation as useful output energy from the device and consider the total input energy to the plant as the amount of recovered hot gas energy.

2.3. Exergy analysis

According to the definition of exergy, it refers to the maximum practical work obtainable from a device or energy stream when it reaches equilibrium with its environment. Exergy is also known in terms like "available energy" or "useful energy," highlighting its distinction from unusable energy. In simpler terms, the total energy of an organism can be categorized into two parts: exergy, the useable portion that can perform work, and energy, the unusable portion that is ultimately dissipated as waste heat. The total exergy of a stream is determined as [37]:

$$\dot{E}x_{tot} = \dot{E}x_{ki} + \dot{E}x_{ph} + \dot{E}x_{ch} + \dot{E}x_{po} \tag{21}$$

where $\dot{E}x_{ki}$, $\dot{E}x_{ph}$, $\dot{E}x_{ch}$, and $\dot{E}x_{po}$ are kinetic exergy, physical exergy, chemical exergy, and potential exergy. Due to the absence of compositional alterations in the proposed CCHP energy conversion mechanisms, chemical exergy is excluded from the analysis. Kinetic and potential exergy can be omitted because there are no changes between streams' entry changes and their exit times when they exit the stream, and physical exergy is defined as [38,39]:

$$ex_{ph} = [H(T,P_0) - H(T_0,P_0)] - T_0[S(T,P_0) - S(T_0,P_0)] \tag{22}$$

The subscript 0 denote the ambient dead state, a standard reference point for evaluating energy transfers and efficiencies. In exergy balance, some of the process's exergies are permanently destroyed and out of efficiency, unlike energy, which is indestructible. This destruction of exergy is due to the irreversibility of the processes carried out; of course, the role of wasted energy should not be simply ignored. However, the exergy balance equation is as follows [40]:

$$\sum_i \dot{m}_i ex_i - \sum_o \dot{m}_o ex_o = \dot{E}x_Q - \dot{E}x_W + \dot{E}x_D \tag{23}$$

In the above equation, $\dot{E}x_Q$, $\dot{E}x_W$, $\dot{E}x_D$ are the exergy of heat transfer, the exergy of work done, and the exergy of destruction, respectively. They determine as [41]:

$$\dot{E}x_Q = \sum \left(1 - \frac{T_0}{T}\right)\dot{Q} \tag{24}$$

$$\dot{E}x_W = \dot{W} \tag{25}$$

The definitions of fuel and product are used in exergy analysis to analyze each piece of equipment. In this definition, fuel refers to any material and energy stream that enters the unit and is consumed to produce useful exergy output or product. Accordingly, each piece of equipment is considered a control volume and exergy destruction equations are written around them, as shown in Table 3.

Exergy efficiency is defined as follows since cooling, heating, and

Table 4
Cost equations around each piece of equipment.

Component	Capital Investment	Ref.
HRSG	$Z_{HRSG} = 309.14({A_{hrsg}}^{0.85})$	[36]
Turbine	$Z_{Turb} = 3880.5({\dot{W}_{turb}}^{0.7})\left(1+\left(\frac{0.05}{1-\eta_T}\right)^3\right)\left(1+5\,exp\left(\frac{T_{in}-866}{10.42}\right)\right)$	[46]
SPH	$Z_{SPH} = 309.14({A_{SPH}}^{0.85})$	[36]
Pump	$Z_p = (705.48{\dot{W}_p}^{0.71})\left(1+\frac{0.2}{1-\eta_p}\right)$	[43]
DHW	$Z_{DHW} = 309.14({A_{DHW}}^{0.85})$	[36]
Generator	$Z_{HG} = 309.14({A_{HG}}^{0.85})$	[36]
HEX	$Z_{HEX} = 309.14({A_{HEX}}^{0.85})$	[33]
Cond	$Z_{Cond} = 516.62(A_{cond})^{0.6}$	[47]
EX. V	$Z_{EX.\,V} = 37\left(\frac{P_{in}}{P_{out}}\right)^{0.68}$	[47]
Evap	$Z_{Evap} = 309.14({A_{Evap}}^{0.85})$	[36]
Abs	$Z_{Abs} = 16000\left(\frac{A_{Abs}}{100}\right)^{0.6}$	[48]

Table 5
The values of economic constant.

Parameters	Symbols	Unit	Values	Ref.
Maintenance factor	Φ	–	1.06	[49]
Annual operating hours	N	H	7446	[49]
Interest factor	I	%	12	[50]
System lifetime	N	years	20	[51]

Table 6
Cost balance and auxiliary equations applied to each component.

Component	Cost Balance	Auxiliary Equations
HRSG	$\dot{C}_1+\dot{C}_9+\dot{Z}_{HRSG}=\dot{C}_2+\dot{C}_5$	$c_1=0$ $c_1=c_2$
Turbine	$\dot{C}_5+\dot{Z}_{Turb}=\dot{C}_6+\dot{C}_W$	$c_5=c_6$
Space heating	$\dot{C}_6+\dot{C}_{10}+\dot{Z}_{SP}=\dot{C}_7+\dot{C}_{11}$	$c_6=c_7$ $c_{10}=0$
Pump	$\dot{C}_8+\dot{C}_{WP}+\dot{Z}_{Pump}=\dot{C}_9$	$c_{wp}=c_w$
DHW	$\dot{C}_2+\dot{C}_{23}+\dot{Z}_{HW}=\dot{C}_3+\dot{C}_{24}$	$c_3=c_4$
Heat generator	$\dot{C}_3+\dot{C}_{21}+\dot{Z}_{Gen}=\dot{C}_4+\dot{C}_{12}+\dot{C}_{16}$	$\frac{(\dot{C}_{12}-\dot{C}_{21})}{(\dot{E}x_{12}-\dot{E}x_{21})}=\frac{(\dot{C}_{16}-\dot{C}_{21})}{(\dot{E}x_{16}-\dot{E}x_{21})}$ $c_2=c_3$
HEX	$\dot{C}_{16}+\dot{C}_{19}+\dot{Z}_{HEX}=\dot{C}_{17}+\dot{C}_{21}$	$c_{16}=c_{17}$
Cond	$\dot{C}_{12}+\dot{C}_{22}+\dot{Z}_{Cond}=\dot{C}_{13}+\dot{C}_{23}$	$c_{12}=c_{13}$ $c_{22}=0$
EX.V1	$\dot{C}_{13}+\dot{Z}_{EX.V1}=\dot{C}_{14}$	-
Evap	$\dot{C}_{14}+\dot{C}_{25}+\dot{Z}_{Evap}=\dot{C}_{15}+\dot{C}_{26}$	$c_{25}=0$ $c_{16}=c_{17}$
EX.V1	$\dot{C}_{17}+\dot{Z}_{EX.V2}=\dot{C}_{18}$	-
Abs	$\dot{C}_{15}+\dot{C}_{18}+\dot{C}_{27}+\dot{Z}_{Abs}=\dot{C}_{28}+\dot{C}_{19}$	$c_{27}=0\,\frac{(\dot{C}_{15}+\dot{C}_{18})}{(\dot{E}x_{15}+\dot{E}x_{18})}=\frac{(\dot{C}_{19})}{(\dot{E}x_{19})}$

power generation are all produced in the setup [42]:

$$\varepsilon_{Ex}=\frac{\dot{E}x_W+\dot{E}x_{Cooling}+\dot{E}x_{heating}}{\dot{E}x_{in}} \tag{39}$$

The following parameters can be determined:

$$\dot{E}x_{in}=ex_1.\dot{m}_1 \tag{40}$$

$$\dot{E}x_W=\dot{W}_{turb} \tag{41}$$

$$\dot{E}x_{Cooling}=\dot{m}_{25}(ex_{25}-ex_{26}) \tag{42}$$

$$\dot{E}x_{heating}=\dot{m}_{23}(ex_{24}-ex_{23}) \tag{43}$$

2.4. Exergo-economic analysis

As part of the design process for an operational design, an essential factor such as economics must be considered in addition to variables such as efficiency and performance. By analyzing the economics of an organization, it is possible to calculate the cost-benefit ratio and the return on investment of the method, which indicates the cost-effectiveness of the setup's construction and implementation. Exergo-economic analysis is a combination of exergy analysis and financial concepts, designed to provide economic performance indicators for a design. All expenses related to the final product are included in the cost concept. As part of an exergo-economic analysis, the final product cost includes two types of costs: exergy costs for each input stream and non-exergy costs, including equipment purchase costs, operational costs, and maintenance expenses. Definitions show the cost balance equation is as follows [43]:

$$\dot{C}_{p,k}=\dot{C}_{f,k}+\dot{Z}_k \tag{44}$$

where $\dot{C}_{p,k}$, $\dot{C}_{f,k}$, $\dot{Z}_k$ are rate of product cost, fuel cost, and non-exergetic cost for K^{th} unit respectively.

$$\dot{C}_{i,k}=c_{i,k}\dot{E}x_{i,k} \tag{45}$$

Here, $\dot{C}_{i,k}$, $c_{i,k}$, $\dot{E}x_{i,k}$ are cost rate, cost of exergy, and exergy rate for kth stream separately. As a result of the definitions, the equation for cost balance is as follows [35,44]:

$$\sum_p^N \left(c_p\dot{E}x_p\right)_k+c_{q,k}\dot{E}x_{q,k}+\dot{Z}_k=\sum_f^N\left(c_f\dot{E}x_f\right)_k+c_{w,k}\dot{W}_k \tag{46}$$

To this place c_w, c_q are the costs of useful work exergy, the cost of heat transfer exergy, and the formula of capital investment cost are determined as [45]:

$$\dot{Z}_K=\frac{Z_k+\varphi+CRF}{N} \tag{47}$$

$$CRF=\frac{i(i+1)^n}{i(i+1)^n-1} \tag{48}$$

$$\text{Payback Period}=\frac{\sum Z_K}{\sum\left(c_p\dot{E}x_p\right)_k} \tag{49}$$

The variable Z_k represents the capital investment cost of kth equipment, the CRF a capital recovery factor specified as equation (48), and Table 4 explores the relationships between these costs and the performance of all units mentioned. The payback period is determined by dividing the sum of the initial capital expenditure by the annual net cash flow. This metric indicates the time required for a project takes to recover its initial investment.

Table 5 presents the values of the economic constant.

The exergo-economic balance and related equations for each unit component are presented in Table 6.

The DUC for CO_2 gas in the condition that the fuel used is MSW or coal equals 0.024 $/kg, according to the DUS values reported by Ahmadi et al. [52]. In the following equations, 50 and 51 are used to calculate the cost rate of environmental penalty ($\dot{C}_{env}$):

$$\dot{m}_{emission}=\dot{m}_{CO_2} \tag{50}$$

$$\dot{C}_{env}=\dot{m}_{CO_2}\times DUS_{CO_2} \tag{51}$$

Table 7
Equation and specification of an important index for exergo-environmental analysis [53,54].

Index name	Equation	Definition	Eq. No.
Exergo-environmental index	$f_{ei} = \frac{\dot{E}x_{D,total}}{\dot{E}x_{in,tot}}$	f_{ei} Represents the ratio of exergy destruction to exergy input. A lower value indicates less exergy destruction relative to exergy input, which is desirable.	(52)
Exergo-environmental improvement	$\theta_{ei} = \frac{100 f_{ei}}{\varepsilon_{Ex}}$	It represents the inverse proportionality of coefficient f_{ei} to exergetic efficiency. A lower value indicates a lower coefficient f_{ei} or, equivalently, a higher exergetic efficiency.	(53)
Exergo-environmental stability	$f_{es} = \frac{\dot{E}x_{out,tot}}{\dot{E}x_{out,tot} + \dot{E}x_{D,total}}$	*f_{es} is the ratio of exergy destruction to exergy output. Lower values signify a more environmentally friendly system.*	(54)
Exergo-environmental sustainability	$\theta_{est} = \frac{f_{es}}{\theta_{ei}}$	Given the definitions of θ_{ei} and f_{es}, a higher value of this coefficient signifies less exergy degradation and improved exergetic performance of the system.	(55)

Table 8
The present study vs. those of Ref. (Li-Br Water absorption chiller and SRC model).

Parameter	Reference findings	Present study	Error (%)	Ref.
SPC supply/return flow rate (kg/s)	209.6	216	3.05	[34]
Net produced power	449	458.5	2.1	[33]
SPH supply/return flow rate(kg/s)	27.82	28.29	1.6	[33]

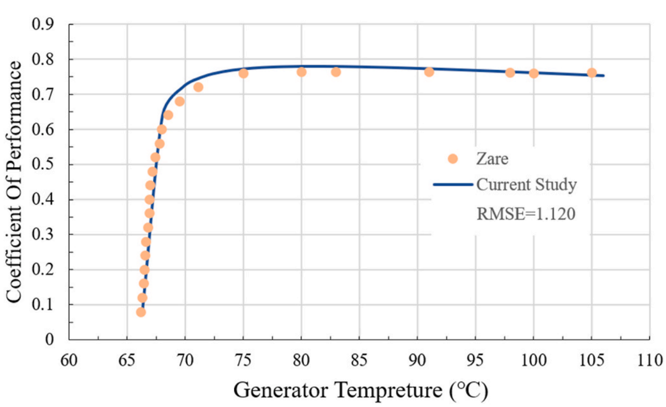

Fig. 3. COP comparison between current study and Zare [34] as a function of generator temperature.

2.5. Exergo-environmental analysis

Prior analyzes of a process only indicated its efficiency and economic factors. An analysis was then conducted to examine a design's environmental impact. Environmental concepts are incorporated into exergy analysis through an exergo-economic analysis, and coefficient numbers have been introduced to represent these impacts somehow. These coefficients calculate equations are presented in Table 7.

Table 9
Thermodynamic properties of each operating stream under the design condition.

Stream Number	Comp.	T_i (°C)	P_i (kPa)	M_i (kg/s)	H_i (kJ/kg)
1	gas, comb	250	101.3	18.43	603.2
2	gas, comb	151.4	101.3	18.43	496.2
3	gas, comb	124.7	101.3	18.43	467.6
4	gas, comb	97.52	101.3	18.43	307.4
5	Steam	145.5	420	0.763	2741
6	Steam	60.06	20	0.763	2373
7	Water	59.96	20	0.763	251
8	Water	59.96	20	0.763	251
9	Water	60.06	420	0.763	251.8
10	Water	25	101.3	18.4	104.9
11	Water	45	101.3	18.4	188.5
12	weak solution Li-Br	80	5.627	0.4203	2650
13	weak solution Li-Br	34.98	5.627	0.4203	146.6
14	weak solution Li-Br	5.001	0.8726	0.4203	146.6
15	weak solution Li-Br	5.002	0.8726	0.4203	2510
16	strong solution Li-Br	80	5.627	4.667	196.5
17	strong solution Li-Br	56.88	5.627	4.667	151.8
18	strong solution Li-Br	56.88	0.8726	4.667	151.8
19	mid solution Li-Br	34.59	0.8726	5.087	87.03
20	mid solution Li-Br	34.69	5.627	5.087	87.23
21	mid solution Li-Br	55.08	5.627	5.087	128.8
22	Water	25	101.3	2.703	104.9
23	Water	32	101.3	2.703	134.2
24	Water	84.66	101.3	2.703	354.6
25	Water	25	101.3	17.37	104.9
26	Water	12	101.3	17.37	50.51
27	Water	25	101.3	6.397	104.9
28	Water	32	101.3	6.397	134.2

Table 10
Energy analysis of the CCHP approach.

Parameters	SRC-based CCHP
Heating Load (kj/s)	2133.9
Cooling Load (kj/s)	945
Net Produced Power (kj/s)	294.9
Total Energy Efficiency (%)	30.2
Total Exergy Efficiency (%)	28.69

2.6. Verification

To verify the CCHP heat recovery cycle, data and reports from Articles 1 and 2 were utilized. These studies explored the application of the CCHP process for heat recovery from diverse sources, explicitly focusing on waste heat utilization from a cement production plant [33] and geothermal sources [34]. Due to the employment of identical data and inputs for the CCHP and the shared EES software information library, the obtained results exhibit a high degree of consistency, key indicators summarized in Table 8. The Coefficient of Performance (COP) is a metric that quantifies the efficiency of a system. It is defined as the ratio of the useful energy output to the total energy input. In the specific case of an absorption chiller, the cooling capacity represents the useful energy output. The total energy input, as detailed in equation (56), consists of the thermal energy supplied to the system and the work expended by the pump to elevate the pressure.

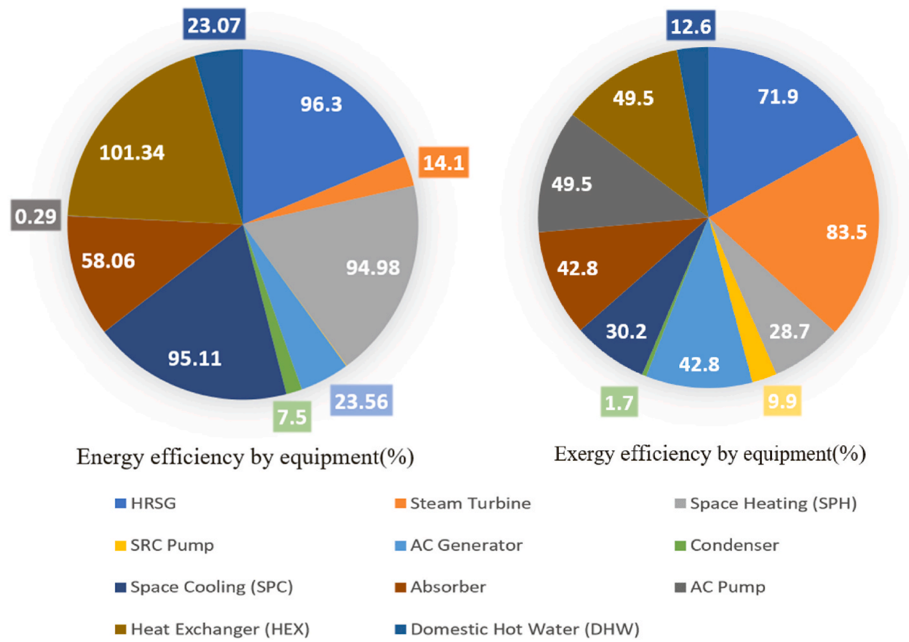

Fig. 4. The comparison of energy and exergy efficiency between different components.

Table 11
Exergo-economic analysis results of the proposed setup.

Item	Symbol	Value
Total cost of purchasing equipment ($)	$Z_{total\ purchasing}$	661803
Total products cost rate ($/hr)	$\dot{C}_{P,total}$	14.45
Cost rate of heating and cooling output ($/hr)	$\dot{C}_{P,heating\ and\ cooling}$	3.846
Cost rate of electricity generation ($/hr)	$\dot{C}_{P,electricity}$	10.6
Cost rate of environmental penalty ($/hr)	$\dot{C}_{env}$	358.27
Payback period (year)	PB	6.183

$$COP = \frac{\dot{Q}_{cooling}}{\dot{Q}_{heating} + \dot{W}_{pump}} \tag{56}$$

To assess the accuracy of the developed absorption chiller model, a direct comparison was made with experimental data from a reference study. The model was operated under identical conditions, including pressures of 5.627 and 0.8726 kPa, a mass flow rate of 22.39 kg/s, and a weak solution composition of 55.28 %. Fig. 3 illustrates the comparison of the coefficient of performance (COP) obtained in this study with the corresponding values reported in the reference study. The data illustrates the COP of absorption chiller as a function of the generator temperature. According to the results, the root mean square error (RMSE) value, which indicates the error level in the proposed model, is 1.2, suggesting an acceptable level of accuracy.

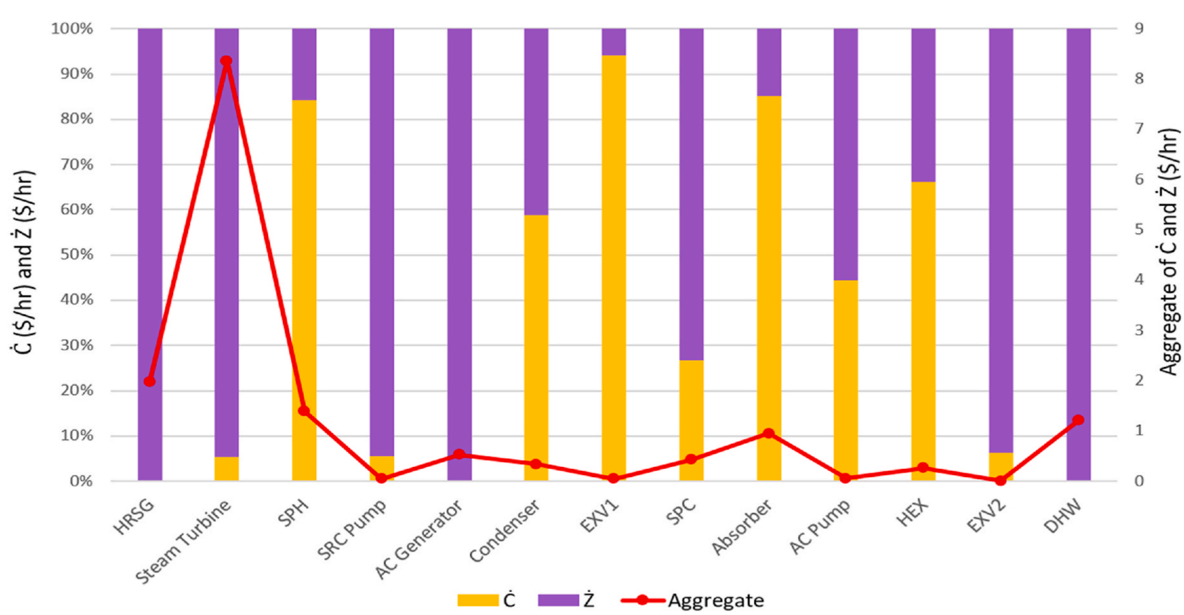

Fig. 5. The cost importance for each devise in heat recovery process.

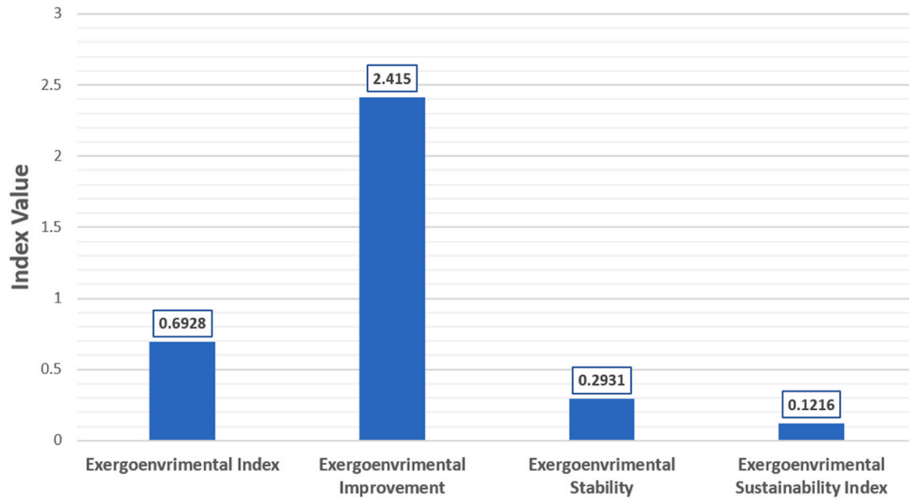

Fig. 6. Exergo-Environmental Performances of proposed CCHP unit.

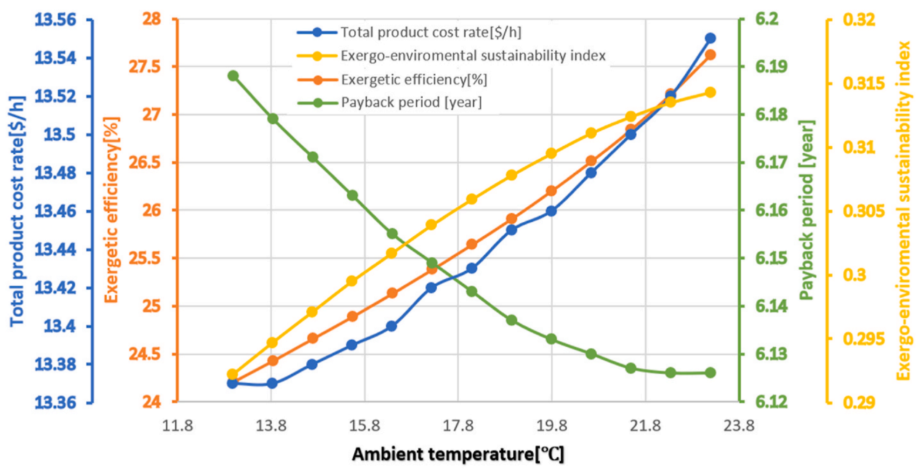

Fig. 7. Effects of varying ambient temperature on Exergetic efficiency, Payback period, Total product cost rate and Exergo-environmental sustainability index.

3. Result and discussion

This section delves into the thermodynamic, exergo-economic, and exergo-environmental analyses of a waste heat recovery approach within a cement plant. The thermodynamic analysis evaluates the energy performance of critical components, such as the Heat Recovery HRSG and turbine, utilizing the EES for simulation. The results highlight the system's efficiency and identify areas for enhancement. The exergo-economic analysis examines the financial implications, including equipment costs and payback periods. During the exergo-environmental analysis, the CO_2 emissions and consequences are analyzed.

3.1. Results of thermodynamic analysis

The energy analysis aims to evaluate the energy performance of the waste heat recovery approach in the cement plant, focusing on the components involved, such as the Heat Recovery Steam Generator (HRSG), turbine, pumps, and other equipment. The goal is to determine how effectively energy is converted and utilized in the modeling. The Engineering Equation Solver (EES) is a powerful software tool designed for solving complex arrangements of simultaneous non-linear equations, particularly in thermodynamics and heat transfer. In the context of Combined Cooling, Heating, and Power (CCHP) approaches, EES can be utilized to simulate the performance of various configurations, such as Steam Rankine Cycle (SRC) units. Several fluids are represented, including gas combustion products, steam, water, and lithium bromide (Li-Br) solutions of varying concentrations (weak, strong, and mid). The temperatures range from 5 °C to 250 °C, pressures from 0.87 kPa to 420 kPa, mass flow rates from 0.42 kg/s to 18.43 kg/s, and specific enthalpies from 50.5 kJ/kg to 2741 kJ/kg. The configuration streams' initial features are presented in Table 9.

The energy analysis evaluates the performance of SRC and its components, focusing on how effectively energy is utilized. Key findings are summarized in Table 10, which includes energy production rates and overall arrangement efficiencies.

The energy analysis of the CCHP model highlights the importance of optimizing the balance between power generation, space heating, space cooling, and domestic hot water production to achieve the highest overall efficiency. The results also emphasize the need to minimize losses in the various components to improve the overall performance of the CCHP installation. The energy analysis reveals that the turbine and SPC have an efficiency of 14.11 % and 95.11 %, respectively. The SPH converts the excess heat from the SRC turbine to useable heat in buildings. The energy analysis indicates that the SPH receives 1811 kW of heat, which is then sent to 1538 kW of users.

Exergy analysis is a powerful tool for assessing the performance and efficiency of energy networks. It provides insights into the quality of energy and identifies where irreversibility and losses occur within the procedure. This section presents a detailed exergy analysis of the framework provided by Combined Cooling, Heating, and Power. The

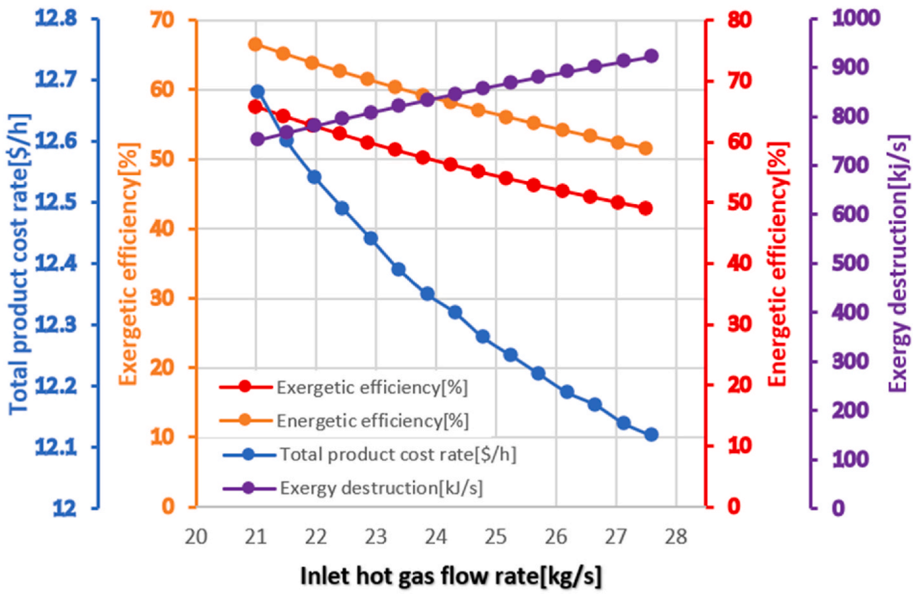

(A)

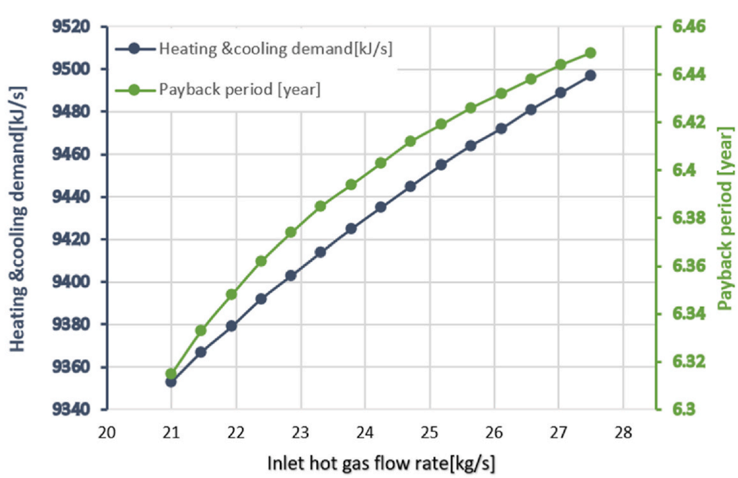

(B)

Fig. 8. Effects of inlet hot gas flow rate changes on Exergetic and Energetic efficiency, Total product cost rate and Exergy destruction in (A) and Heating and cooling demand and Payback period in (B).

analysis focuses on the exergy flows, destruction, and efficiencies of each significant component, highlighting areas for potential improvement. The overall exergy efficiency of the CCHP method is 28.69 %, with the HRSG and steam turbine being the most efficient components. The analysis reveals that, while the organization can effectively convert a portion of the input exergy into valuable outputs, there are significant losses in SPH, SPC, and DHW. The SPH and the absorber exhibit low exergy efficiencies, indicating substantial exergy destruction. The SPC approach has an exergy efficiency of 30.2 %, while the absorber operates at 42.8 % efficiency. The inefficiencies in these components are primarily due to temperature mismatches and inherent irreversibility in the cooling processes. These components collectively illustrate a well-designed thermodynamic technique that maximizes energy utilization while minimizing waste, laying a solid foundation for further enhancements and sustainability initiatives. Fig. 4 presents a visual comparison of energy and exergy efficiency for various components within a CCHP method, making it easy to compare efficiencies and identify areas for improvement.

3.2. Results of exergo-economic and exergo-environmental analysis

Exergo-economic analysis was done to examine the financial benefits. The essential parameters for the cost-effectiveness evaluation of cement plant waste heat recovery are reported in Table 11. The total fixed costs due to the purchase of equipment were 661,803 $, the highest cost related to the HRSG unit and is equal to 103,490 $. According to the calculations based on the exergy unit, the total product cost rate, heating and cooling output cost rate, and electricity generated cost rate by the recovery arrangement are 14.45 $/hr, 3.846 $/hr, and 10.6 $/hr, respectively. By obtaining the ratio of the total cost of purchasing process equipment to the annual income from the heat recovery process, the payback period can be estimated at 6.2 years. In this study, based on the

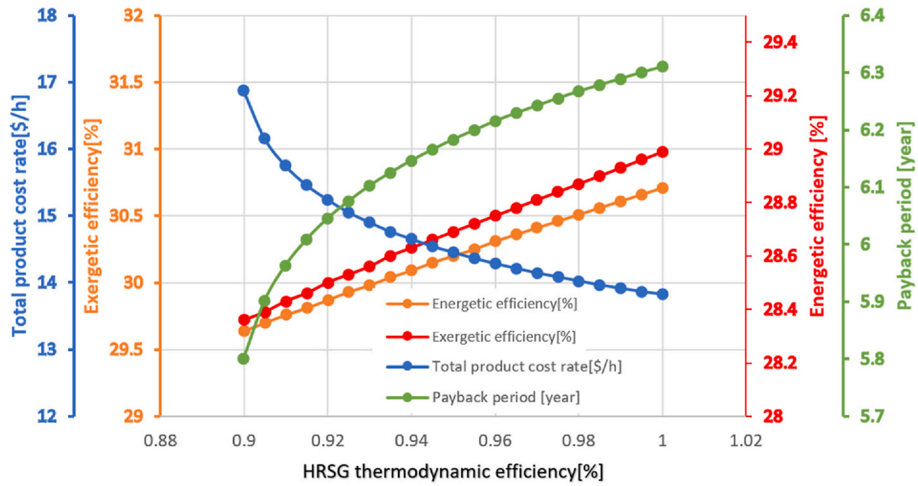

(A)

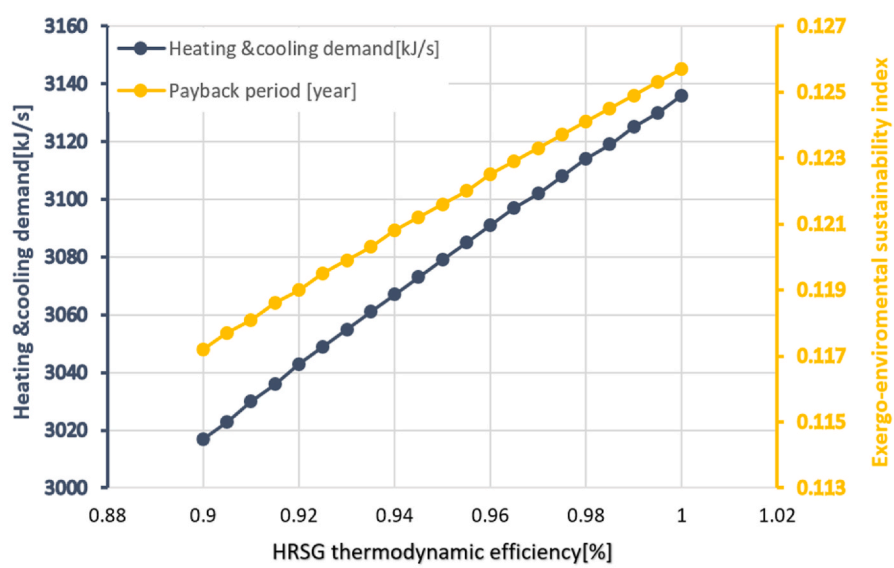

(B)

Fig. 9. Effects of HRSG thermodynamic efficiency on Exergetic and Energetic efficiency, Payback period, and Total product cost rate in (A) and Heating and cooling demand and Exergo-environmental sustainability index (B).

amount of CO_2 emissions and DUC, the cost rate of environmental penalty is estimated at 358.27 $/hr.

Two of the critical and influential factors in exergo-economic analysis are the examination of the cost of exergy destruction and the amount of cost that must be paid for the purchase of each piece of equipment per hour. In this way, the values of the total cost rate of exergy destruction ($\dot{C}_D$) and the total cost rate of purchasing equipment ($\dot{Z}_K$) were calculated as 2.981 and 12.61. The amount of $\dot{C}_D$ and $\dot{Z}_K$ and the sum of these two parameters is shown as cost importance in the diagram of Fig. 5. Equipment such as SPH, SPC, absorber, and HEX has high $\dot{C}_D$ due to high exergy destruction. On the other hand, equipment like HRSG and AC generators, for which the cost of feed is zero, have a zero value of $\dot{C}_D$. Converting a large volume of steam into energy per hour by the turbine causes a large amount of $\dot{Z}_K$. Also, high heat transfer in HRSG requires a high contact surface, which justifies the high purchase cost rate.

The investigation of the environmental effects of the process was carried out by determining those damages that are expressed due to method inefficiency under the title exergo-environmental index, and its value was calculated as 0.6928. The amount of environmental damage caused by this study is estimated at 2.415. Exergo-environmental stability and exergo-environmental sustainability index were calculated as 0.2931 and 0.1216, respectively, as shown in Fig. 6.

3.3. Evaluation of output sensitivity to input parameter fluctuations

In this section, the response of the CCHP thermodynamic model to heat recovery from waste hot gas in the cement industry is analyzed. This analysis aims to investigate the impact of changes in various independent variables on the critical results of the structure. Using the information presented in this section, appropriate decisions can be made to modify the planning and improve its results and efficiency. In other words, this analysis is designed to increase energy efficiency and reduce

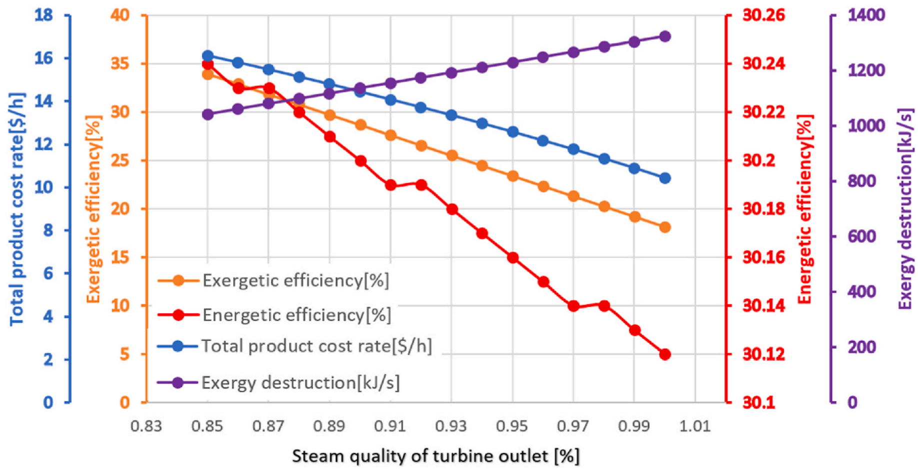

(A)

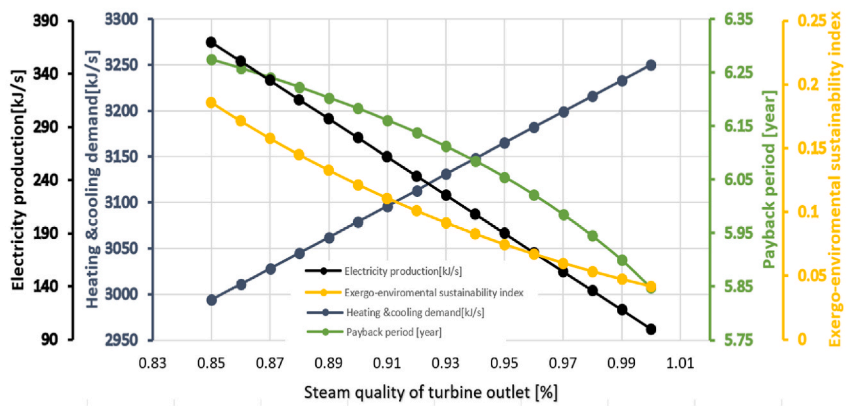

(B)

Fig. 10. Effects of varying steam quality of turbine outlet on Exergetic and Energetic efficiency, Total product cost rate and Exergy destruction in (A) and Heating and cooling demand, Payback period, Electricity production and Exergo-environmental sustainability index (B).

operating costs.

Fig. 7 presents an analysis of the influence of varying ambient temperature, a crucial input parameter in exergy analysis, on key performance indicators such as payback period and final product cost. Since outdoor temperatures change throughout the year and day, we can study how this affects strategy performance. As ambient temperature rises, exergy efficiency increases, narrowing the exergy gap relative to the dead state. This correlation results in enhanced overall plant efficiency. Correspondingly, the total product cost increases at a comparable rate. However, the payback period diminishes at a more pronounced pace with an increasing total product cost rate. Small changes in equipment costs have a much more significant impact on overall investment than on the total product cost rate.

Cement plants exhibit diverse production capacities, leading to variations in fuel consumption and, consequently, the characteristics of their waste heat streams. Fig. 8 examines the impact of varying inlet hot gas flow rates on the process. When the inlet gas flow rate increases, both energy and exergy efficiencies typically decline at 17.1 % and 14.6 %. This is attributed to the model's limited heat recovery capacity, which cannot keep pace with the augmented gas flow. Moreover, the increased gas flow rate results in higher exergy destruction, leading to a lower total product cost and, consequently, a more extended payback period. The payback period is projected to reach 6.45 years, primarily due to the increased production of heating, cooling, and electricity.

Fig. 9 demonstrates that as the HRSG efficiency increases and approaches its ideal state, both energy and exergy efficiencies improve. This enhancement is attributed to a 130 kJ/s increase in heating and cooling production. However, due to the decreasing total product cost rate, the payback period lengthens by approximately 0.5 years, which is undesirable. These changes result from improved heat transfer within the HRSG, leading to a higher heat load on the SRC components and, consequently, reduced heat loads on the subsequent sections. This results in increased electricity generation and heat production in the SPH but decreased heating and cooling in the AC and DHW parts, respectively.

Fig. 10 demonstrates that as the quality of steam exiting the turbine increases, a decrease in electricity generation occurs. As less steam is converted to liquid, less energy is converted into electricity, resulting in a decrease in the total product cost rate from 16.13 $ to 10.45 $. Moreover, due to changes in production and alterations in the quality of steam exiting the turbine, the unit payback period decreases, highlighting the significance of this equipment in the overall design and its ability to induce substantial changes. Given that the components' heating and cooling production has increased and that the most exergy destruction occurs in the equipment associated with heat transferring processes, the decrease in the exergo-environmental index from nearly 0.2 to 0.04 is justifiable. It is important to note that as the turbine exhaust gas becomes more saturated and electricity production

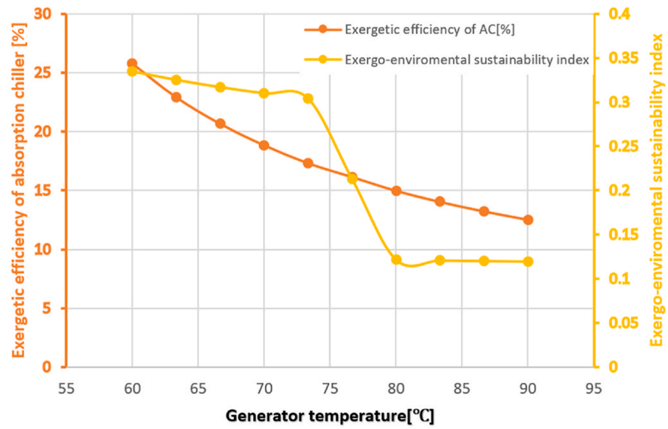

(A)

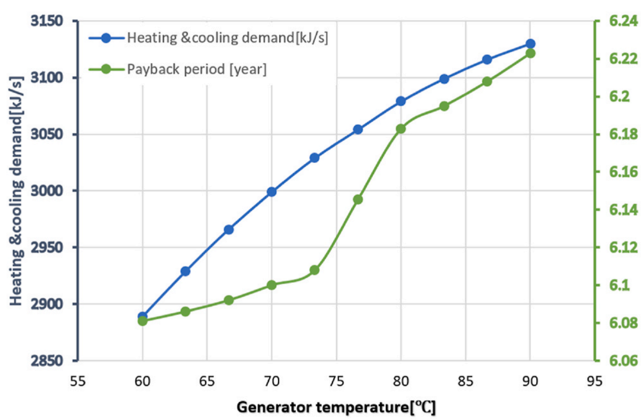

(B)

Fig. 11. Effects of generator temperature changes on Exergetic efficiency of AC, Exergo-environmental sustainability index, Heating and cooling demand and Payback period.

increases, the turbine is subject to higher wear and tear, necessitating earlier-than-expected maintenance or replacement costs.

Another critical component whose variations have significant impacts is the generator. Fig. 11 illustrates the results of temperature changes in the generator, by increasing the generator temperature from 60 to 90 °C, cooling production increases, as shown in the figure. Due to the increased temperature of the outlet streams from the generator (streams 12 and 16), the heat output in the condenser also increases. This enhances the preheating of stream 22 and provides a suitable heat load for the inlet stream to the DHW. However, due to the increased exergy destruction from 1043 to 1324 kJ/s at higher temperatures, the exergo-environmental sustainability index of the procedure decreases in the amount of 0.21, impacting its sustainability.

One of the fundamental data points that directly impacts the equipment's costs is the high and low pressures in the SRC and AC modules. Fig. 12 shows that increasing the upper and lower pressure of the SRC cycle enhances the exergy efficiency within the same sub-assembly and increases the total product cost rate. This is because increasing the high pressure allows for injecting steam with a higher heat load into the turbine, affecting the heat generated by the SPC. Moreover, increasing the condenser's pressure reduces the pump work, and increasing the pump's outlet pressure is also beneficial for the payback period, reducing it. However, changes in this parameter at lower condenser pressures occur with a steeper slope. Fig. 13 demonstrates that increasing the pump's outlet pressure leads to an increase in both the total product cost rate and the Exergo-environmental sustainability index. However, these changes occur with a steeper slope at lower pressures. For instance, at a pressure of 10 kPa, the change in the final product price is approximately 1.9 $/s.

Increasing the upper and lower pressures of the absorption chiller cycle results in a decrease in exergy efficiency and a rise in the total product cost rate, as shown in Figs. 14 and 15. This change is attributed to the increased pump work associated with higher HEX's pressures, although this effect is less significant than changing the SPC pressure. This is because the saturation temperature is lower at SPC's pressures, leading to a more considerable temperature difference across the SPC, which is the most efficient part of the operation. Additionally, the increased pump work contributes to the higher cost. Increasing upper and lower pressures within the absorption chiller cycle diminishes exergy efficiency and elevates the total product cost rate. The primary reason for this is the augmented pump work necessitated by higher HEX pressures; however, alterations in SPC's pressure exert a more pronounced influence. This is attributed to the lower saturation temperature at reduced pressures, resulting in a wider temperature differential across the SPC, the section's most crucial component. Moreover, the increased pump work exacerbates the cost increase. This is due to changes in exergy, cooling, and heating production, as well as equipment purchase costs. The decrease in exergy destruction positively impacts the exergo-environmental sustainability index.

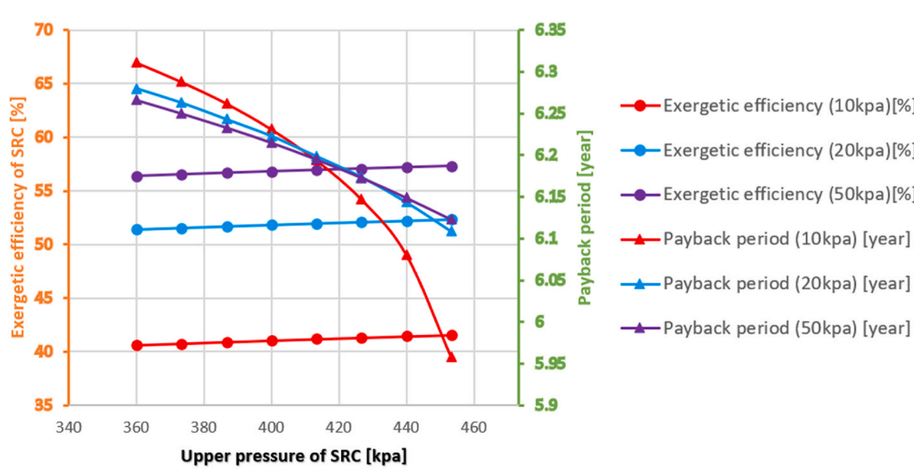

Fig. 12. Effects of upper and lower pressure of SRC cycle changes on Exergetic efficiency and Payback period.

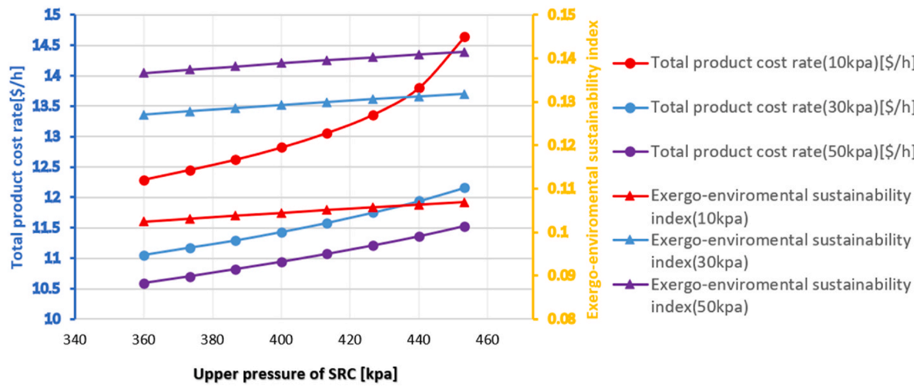

Fig. 13. Effects of upper and lower pressure of SRC cycle changes on Total product cost rate and Exergo-environmental sustainability index.

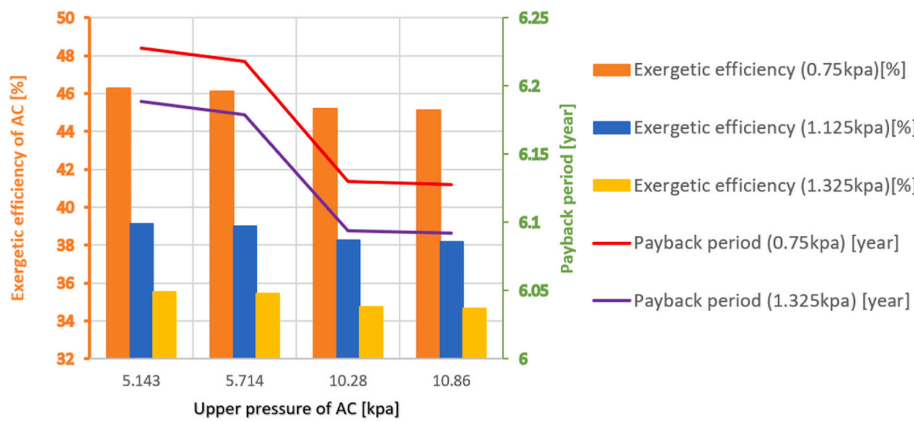

Fig. 14. Effects of upper and lower pressure of SRC cycle changes on Exergetic efficiency and Payback period.

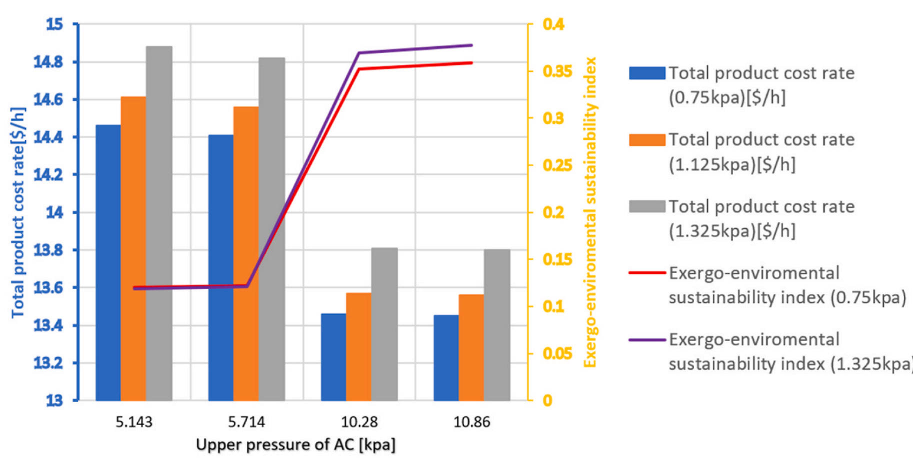

Fig. 15. Effects of upper and lower pressure of SRC cycle changes on Total product cost rate and Exergo-environmental sustainability index.

4. Conclusion

This study investigated the integration of a CCHP system into the cement industry to enhance energy efficiency and reduce greenhouse gas emissions. The CCHP system, designed to recover waste heat from the clinker production process, demonstrated Significant potential for improving the overall system's energy and exergy performance.

Energy and Exergy Analysis.

- The CCHP system exhibited a total energy efficiency of 30.2 % and an exergy of 28.69 %.
- Key areas for improvement to maximize energy recovery were identified, particularly in the Heat Recovery Steam Generator (HRSG) and turbine.

Economic and Environmental Analysis.

- The proposed CCHP system presented a promising economic feasibility, with a payback period of 6.18 years.
- The exergo-environment sustainability index of 0.12 indicated a relatively sustainable operation.

Sensitivity Analysis.

- Increased ambient temperature and inlet hot gas flow rate generally led to improved exergetic efficiency and reduced payback period, albeit with increased energy consumption and exergy destruction.
- Enhancing HRSG efficiency resulted in shorter payback periods, lower total product cost, and increased heating and cooling demands.
- Higher turbine steam quality led to reduced energy conversion efficiency and increased exergy destruction, negatively impacting the system's performance. Increasing generator temperature resulted in decreased exergetic efficiency and longer payback periods.
- Adjusting the pressure in the SRC and AC cycles influenced the system's performance, with potential trade-offs between efficiency, cost, and environmental impact.

4.1. Limitations and future research directions

Limitations include the reliance on fixed operational parameters, which may not account for real-world fluctuations in input gas flow or ambient temperatures. Additionally, the system's performance may vary with changes in pressure settings and component efficiencies, highlighting areas for further optimization.

Future work could explore dynamic simulations to accommodate varying operational conditions and investigate alternative configurations for enhanced exergy efficiency. Additionally, exploring renewable energy integration, such as solar or biomass, could further reduce environmental impact and support long-term sustainability goals in cement manufacturing.

CRediT authorship contribution statement

Mahdi Mahmoudkhani: Writing – original draft, Software, Methodology. **Alibakhsh Kasaeian:** Writing – review & editing, Conceptualization. **Narges Sadat Nazari:** Writing – original draft, Validation. **Fatemeh Afshari:** Investigation. **Mehdi Esmaeili Bidhendi:** Supervision, Resources.

Declaration of competing interest

The authors declare that they have no known competing financial interests or personal relationships that could have appeared to influence the work reported in this paper.

Data availability

Data will be made available on request.

References

[1] Ali MB, Saidur R, Hossain MS. A review on emission analysis in cement industries. Renew Sustain Energy Rev 2011;15(5):2252–61.
[2] Nazari N, et al. Optimization of carbon dioxide adsorption from industrial flue gas using zeolite 13X: a simulation study with aspen adsorption and response surface methodology. Results in Engineering 2024:103206.
[3] Sabuz MZ, et al. Environment sustainability practices in bangladeshi cement industries. Journal of Engineering Research 2021. https://doi.org/10.36909/jer.ICETET.14995.
[4] Barghamadi H, et al. Thermodynamic evaluation of a novel open volumetric receiver-heliostat plant/desalination unit hybrid system. Desalination 2024;577:117367.
[5] Pili R, et al. Techno-economic potential of waste heat recovery from German energy-intensive industry with Organic Rankine Cycle technology. Renew Sustain Energy Rev 2020;134:110324.
[6] Ishaq H, Dincer I, Naterer GF. Exergy and cost analyses of waste heat recovery from furnace cement slag for clean hydrogen production. Energy 2019;172:1243–53.
[7] Mohammadi A, et al. Thermodynamic analysis of a combined gas turbine, ORC cycle and absorption refrigeration for a CCHP system. Appl Therm Eng 2017;111:397–406.
[8] Agathokleous R, et al. Waste Heat Recovery in the EU industry and proposed new technologies. Energy Proc 2019;161:489–96.
[9] Tashtoush B, et al. Exergoeconomic analyses of a cement plant waste heat recovery in a novel combined power and refrigeration cycle. Int J Des Nat Ecodyn 2021;16:251–60.
[10] Ige OE, Von Kallon DV, Desai D. Carbon emissions mitigation methods for cement industry using a systems dynamics model. Clean Technol Environ Policy 2024;26(3):579–97.
[11] Mirzaei MR, et al. Thermo-economic analysis of an integrated combined heating, cooling, and power unit with dish collector and organic Rankine cycle. Energy 2024;296:131089.
[12] Ganapathiraju V, Srinivas T. Power-augmented steam power plant in a cogeneration cement factory. J Energy Eng 2016;143:04016020.
[13] Ghalandari V, Majd MM, Golestanian A. Energy audit for pyro-processing unit of a new generation cement plant and feasibility study for recovering waste heat: a case study. Energy 2019;173:833–43.
[14] Chen H, et al. Performance evaluation of a novel design for the waste heat recovery of a cement plant incorporating a coal-fired power plant. Energy 2022;246:123420.
[15] Hamedi Jamali D, Noorpoor A. Optimization of a novel solar-based multi-generation system for waste heat recovery in a cement plant. J Clean Prod 2019;240:117825.
[16] Brückner S, et al. Industrial waste heat recovery technologies: an economic analysis of heat transformation technologies. Appl Energy 2015;151:157–67.
[17] Han T, et al. Optimization of waste heat recovery power generation system for cement plant by combining pinch and exergy analysis methods. Appl Therm Eng 2018:140.
[18] Khurana S, Banerjee R, Gaitonde U. Energy balance and cogeneration for a cement plant. Appl Therm Eng 2002;22:485–94.
[19] Tang Y, et al. Multi-mode operation of a novel dual-pressure steam rankine cycle system recovering multi-grade waste heat from a marine two-stroke engine equipped with the high-pressure exhaust gas recirculation system. Energy 2024;301:131675.
[20] Gomaa MR, et al. Experimental investigation on waste heat recovery from a cement factory to enhance thermoelectric generation. Sustainability 2022;14. https://doi.org/10.3390/su141610146.
[21] Lu P, et al. Design and optimization of organic rankine cycle based on heat transfer enhancement and novel heat exchanger: a review. Energies 2023;16. https://doi.org/10.3390/en16031380.
[22] Ahmed A, et al. Design methodology of organic Rankine cycle for waste heat recovery in cement plants. Appl Therm Eng 2018;129:421–30.
[23] Ozturk M, Dincer I. Utilization of waste heat from cement plant to generate hydrogen and blend it with natural gas. Int J Hydrogen Energy 2022;47(48):20695–704.
[24] Freeman J, et al. A small-scale solar organic Rankine cycle combined heat and power system with integrated thermal-energy storage. Appl Therm Eng 2017:127.
[25] Karellas S, et al. Energetic and exergetic analysis of waste heat recovery systems in the cement industry. Energy 2013;58:147–56.
[26] Østergaard PA, et al. Renewable energy for sustainable development. Renew Energy 2022;199:1145–52.
[27] Hai T, et al. Multiobjective optimization of a cogeneration system based on gas turbine, organic rankine cycle and double-effect absorbtion chiller. Chemosphere 2023;338:139371.
[28] Nami H, Anvari-Moghaddam A, Arabkoohsar A. Application of CCHPs in a centralized domestic heating, cooling and power network—thermodynamic and economic implications. Sustain Cities Soc 2020;60:102151.
[29] Wang Y., et al. A novel carbon dioxide capture system for a cement plant based on waste heat utilization. SSRN Electron J 2021.Energy Conversion and Management, Volume 257, 2022, 115426, ISSN 0196-8904.
[30] Wang J, et al. Energy, exergy, exergoeconomic and environmental (4E) analysis of a distributed generation solar-assisted CCHP (combined cooling, heating and power) gas turbine system. Energy 2019;175:1246–58.
[31] Ustaoglu A, Alptekin M, Akay ME. Thermal and exergetic approach to wet type rotary kiln process and evaluation of waste heat powered ORC (Organic Rankine Cycle). Appl Therm Eng 2017;112:281–95.
[32] Liu E, et al. Waste heat recovery and utilization of cement rotary kiln based on biomass energy. Bioresources 2023;18:3056–72.
[33] Nami H, Anvari-Moghaddam A. Small-scale CCHP systems for waste heat recovery from cement plants: thermodynamic, sustainability and economic implications. Energy 2020;192:116634.
[34] Zare V. A comparative thermodynamic analysis of two tri-generation systems utilizing low-grade geothermal energy. Energy Convers Manag 2016;118:264–74.
[35] Bejan A, Tsatsaronis G, Moran MJ. Thermal design and optimization. John Wiley & Sons; 1995.
[36] Din I, Rosen MA, Ahmadi P. Optimization of energy systems. John Wiley & Sons; 2017.
[37] Ghorbani S, et al. Parametric study and optimization of a novel geothermal-driven combined cooling, heating, and power (CCHP) system. Energy 2023;263:126143.
[38] Rad EA, Mohammadi S, Tayyeban E. Simultaneous optimization of working fluid and boiler pressure in an organic Rankine cycle for different heat source temperatures. Energy 2020;194:116856.
[39] Pantaleo AM, et al. Hybrid solar-biomass combined Brayton/organic Rankine-cycle plants integrated with thermal storage: techno-economic feasibility in selected Mediterranean areas. Renew Energy 2020;147:2913–31.

[40] Emadi MA, et al. Working-fluid selection and thermoeconomic optimisation of a combined cycle cogeneration dual-loop organic Rankine cycle (ORC) system for solid oxide fuel cell (SOFC) waste-heat recovery. Appl Energy 2020;261:114384.
[41] Dincer I, Rosen MA. Energy, environment and sustainable development. Applied energy 1999;64(1–4):427–40.
[42] Özdemir A, Gamze G. A comprehensive comparative energy and exergy analysis in solar based hydrogen production systems. Int J Hydrogen Energy 2022;47(24): 12189–203.
[43] Hashemian N, Noorpoor A. A geothermal-biomass powered multi-generation plant with freshwater and hydrogen generation options: thermo-economic-environmental appraisals and multi-criteria optimization. Renew Energy 2022; 198:254–66.
[44] Habibollahzade A, Mehrabadi ZK, Markides CN. Comparative thermoeconomic analyses and multi-objective particle swarm optimization of geothermal combined cooling and power systems. Energy Convers Manag 2021;234:113921.
[45] Manesh MHK, et al. Techno-economic, environmental and emergy analysis and optimization of integrated solar parabolic trough collector and multi effect distillation systems with a combined cycle power plant. Energy 2022;240:122499.
[46] Ghasemi A, Heidarnejad P, Noorpoor A. A novel solar-biomass based multi-generation energy system including water desalination and liquefaction of natural gas system: thermodynamic and thermoeconomic optimization. J Clean Prod 2018; 196:424–37.
[47] Peters MS, Timmerhaus KD. Plant design and economics for chemical engineers. (No Title). 1968.
[48] Ebrahimi-Moghadam A, Farzaneh-Gord M. A sustainable optimal biomass waste-driven CCHP system to boost the nearly zero energy building concept. Energy Convers Manag 2023;277:116669.
[49] Khanmohammadi S, Azimian AR. Exergoeconomic evaluation of a two-pressure level fired combined-cycle power plant. J Energy Eng 2015;141(3):04014014.
[50] Ahmadi P, Dincer I. Thermodynamic and exergoenvironmental analyses, and multi-objective optimization of a gas turbine power plant. Appl Therm Eng 2011; 31(14–15):2529–40.
[51] Köse Ö, Koç Y, Yağlı H. Energy, exergy, economy and environmental (4E) analysis and optimization of single, dual and triple configurations of the power systems: rankine Cycle/Kalina Cycle, driven by a gas turbine. Energy Convers Manag 2021; 227:113604.
[52] Barzegar Avval H, et al. Thermo-economic-environmental multiobjective optimization of a gas turbine power plant with preheater using evolutionary algorithm. Int J Energy Res 2011;35(5):389–403.
[53] Ratlamwala TA, Dincer I, Gadalla MA. Comparative environmental impact and sustainability assessments of hydrogen and cooling production systems. Causes, impacts and solutions to global warming 2013:389–408.
[54] Ratlamwala TA, Dincer I, Reddy BV. Exergetic and environmental impact assessment of an integrated system for utilization of excess power from thermal power plant. Causes. In: Impacts and solutions to global warming; 2013. p. 803–24.